

A Comparison of BRDF Representations and their Effect on Signatures

October 1998

James Jafolla
Surface Optics Corporation
San Diego, CA 92127

David Thomas
U.S. Tank-Automotive and Armaments Command
Warren, MI 48397

John Hilgers
Signature Research, Inc.
Calumet, MI 49913

ABSTRACT

The application of advanced low observable treatments to ground vehicles has led to a requirement for a better understanding of effects of light scattering from surfaces. Measurements of the Bidirectional Reflectance Distribution Function (BRDF) fully describe the angular scattering properties of materials, and these may be used in signature simulations to accurately characterize the optical effects of surface treatments on targets. This paper examines some of the popular parameterized BRDF representations and shows their effect on signature calculations.

1.0 INTRODUCTION

The application of BRDF data in signature analysis to obtain visually realistic images and radiometric accuracy for system effectiveness evaluation is ongoing issue for the modeling and simulation community. Most commercial visualization implementations use a simple specular/diffuse approximation to the surface optical properties. Even the more sophisticated signature analysis codes often resort to simplified, parameterized representations of the actual BRDF. The introduction of BRDF data into signature analysis raises a number of technical questions. How much BRDF data is required, and what is the necessary spectral and angular resolution? What requirements does this impose on the geometry model? What is the best way of representing BRDF data for accurate signature calculations?

We will attempt to answer some of these questions by comparing BRDF measurements to parameterized representations of the BRDF. Additional BRDF data is compared to the BRDF predictions for stressing geometries (i.e., high angles of incidence and reflection) to assess the parameterized BRDF model accuracy. In addition, signature analysis is performed on simple geometries to assess the radiometric effects of these BRDF approximations.

REPORT DOCUMENTATION PAGE				Form Approved OMB No. 0704-0188	
Public reporting burden for this collection of information is estimated to average 1 hour per response, including the time for reviewing instructions, searching existing data sources, gathering and maintaining the data needed, and completing and reviewing this collection of information. Send comments regarding this burden estimate or any other aspect of this collection of information, including suggestions for reducing this burden to Department of Defense, Washington Headquarters Services, Directorate for Information Operations and Reports (0704-0188), 1215 Jefferson Davis Highway, Suite 1204, Arlington, VA 22202-4302. Respondents should be aware that notwithstanding any other provision of law, no person shall be subject to any penalty for failing to comply with a collection of information if it does not display a currently valid OMB control number. PLEASE DO NOT RETURN YOUR FORM TO THE ABOVE ADDRESS.					
1. REPORT DATE (DD-MM-YYYY) 01-10-1998		2. REPORT TYPE Conference Proceedings		3. DATES COVERED (FROM - TO) xx-xx-1998 to xx-xx-1998	
4. TITLE AND SUBTITLE A Comparison of BRDF Representations and their Effect on Signatures Unclassified				5a. CONTRACT NUMBER	
				5b. GRANT NUMBER	
				5c. PROGRAM ELEMENT NUMBER	
6. AUTHOR(S) Jafolla, James ; Thomas, David ; Hilgers, John ;				5d. PROJECT NUMBER	
				5e. TASK NUMBER	
				5f. WORK UNIT NUMBER	
7. PERFORMING ORGANIZATION NAME AND ADDRESS Surface Optics Corporation San Diego, CA92127				8. PERFORMING ORGANIZATION REPORT NUMBER	
9. SPONSORING/MONITORING AGENCY NAME AND ADDRESS Director, CECOM RDEC Night Vision and Electronic Sensors Directorate, Security Team 10221 Burbeck Rd. Ft. Belvoir, VA22060-5806				10. SPONSOR/MONITOR'S ACRONYM(S)	
				11. SPONSOR/MONITOR'S REPORT NUMBER(S)	
12. DISTRIBUTION/AVAILABILITY STATEMENT APUBLIC RELEASE					
13. SUPPLEMENTARY NOTES See Also ADM201041, 1998 IRIS Proceedings on CD-ROM.					
14. ABSTRACT The application of advanced low observable treatments to ground vehicles has led to a requirement for a better understanding of effects of light scattering from surfaces. Measurements of the Bidirectional Reflectance Distribution Function (BRDF) fully describe the angular scattering properties of materials, and these may be used in signature simulations to accurately characterize the optical effects of surface treatments on targets. This paper examines some of the popular parameterized BRDF representations and shows their effect on signature calculations.					
15. SUBJECT TERMS					
16. SECURITY CLASSIFICATION OF:		17. LIMITATION OF ABSTRACT	18. NUMBER OF PAGES	19. NAME OF RESPONSIBLE PERSON	
		Public Release	16	Fenster, Lynn lfenster@dtic.mil	
a. REPORT Unclassified		b. ABSTRACT Unclassified		c. THIS PAGE Unclassified	
				19b. TELEPHONE NUMBER International Area Code Area Code Telephone Number 703767-9007 DSN 427-9007	
				Standard Form 298 (Rev. 8-98) Prescribed by ANSI Std Z39.18	

2.0 BRDF DEFINITION

The function used to describe the directional dependence of the reflected energy is the Bidirectional Reflectance Distribution Function (BRDF). The geometry of the BRDF definition is shown in Figure 1

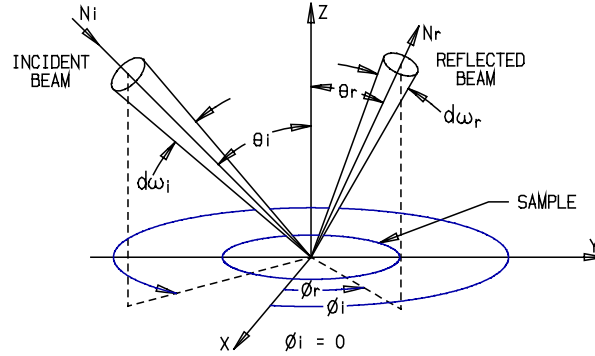


Figure 1 BRDF Geometry.

The BRDF is defined as the ratio of the reflected radiance ($\text{w}\cdot\text{m}^{-2}\cdot\text{sr}^{-1}$) in a particular direction (θ_r, ϕ_r) to the incident irradiance ($\text{w}\cdot\text{m}^{-2}$) from direction (θ_i, ϕ_i) .

$$\rho'(\theta_i, \phi_i, \theta_r, \phi_r) = \frac{\delta N_r(\theta_r, \phi_r)}{N_i(\theta_i, \phi_i) \cos \theta_i \delta \omega_i}$$

The units of the BRDF are inverse solid-angle (sr^{-1}).

Figure 2 shows a pictorial representation of a typical BRDF, taken from the well-known paper by Nicodemus [1] that provides a good physical description of these concepts.

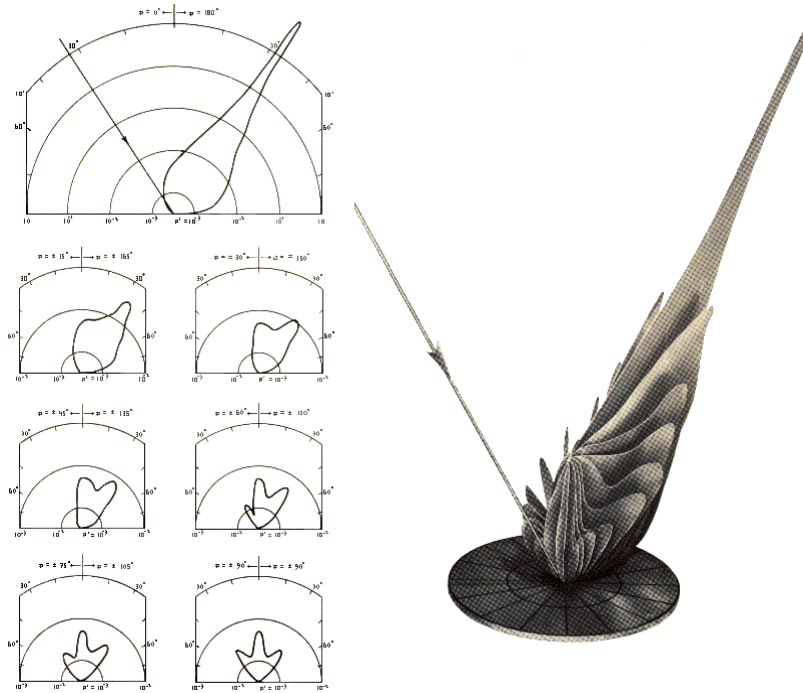


Figure 2 BRDF Visualization from Ref. 1.

The integral of the BRDF over all reflected angles provides the dimensionless Directional Hemispherical Reflectance (DHR). Similarly, the integral of the BRDF over all incident angles gives the Hemispherical Directional Reflectance (HDR). Because the BRDF is invariant under interchange of incident and reflected angles (reciprocity) the HDR and DHR are equivalent, and can be used interchangeably.

3.0 PARAMETERIZED BRDF MODELS

Signature analysis of realistic targets and backgrounds typically specifies a wide variety of materials in the scene. Also, a full spatial and spectral characterization of the BRDF requires a significant data collection effort, and produces a large volume of data. In order to manage the optical database and simplify the computational requirements, a number of parameterized representations of the BRDF have been developed. In this paper, we will examine the fidelity of two BRDF models that are widely used in signature analysis: the Sandford-Robertson [2] four-parameter model and the OPTASM Lorentzian lobe model developed by Acquista and Rosenwald [3].

Sandford-Robertson BRDF model

The Sandford-Robertson (SR) model is based on the assumption that the angular properties of the BRDF vary slowly with wavelength and can be separated from the spectral characteristics.

$$\rho'(\hat{k}_i, \hat{k}_r; \lambda) = f_r(\hat{k}_i, \hat{k}_r) \rho(\lambda)$$

where \hat{k}_i is the unit vector to the light source and \hat{k}_r is the unit vector to the receiver, and $\rho(\lambda)$ is the total spectral reflectance of the surface. It is further assumed the angular dependence can be separated into a specular and diffuse component

$$f_r(\hat{k}_i, \hat{k}_r) = f_D(\hat{k}_i, \hat{k}_r) + f_S(\hat{k}_i, \hat{k}_r)$$

The directional and spectral dependence of the emissivity is used to determine the diffuse scattering parameters, $\varepsilon(\lambda)$ and b , from spectral HDR measurements

$$\begin{aligned} 1 - \rho(\theta, \lambda) &= \varepsilon(\theta, \lambda) \\ &= \varepsilon(\lambda) g(\theta) / G(b) \end{aligned}$$

where $\varepsilon(\lambda)$ is the total spectral emissivity. The grazing angle dependence is given by

$$g(\theta) = 1 / (1 + b^2 \tan^2 \theta)$$

and the normalization constant of the angular distribution is

$$G(b) = \frac{1}{1 - b^2} \left[1 - \frac{b^2}{1 - b^2} \log(1/b^2) \right]$$

The diffuse component of the BRDF is given by

$$f_D(\hat{k}_i, \hat{k}_r) = \frac{1}{\pi} g(\theta_r) \rho_D(\lambda) g(\theta_i) / G^2(b)$$

The specular component of the BRDF lobe is assumed to be a circular ellipsoid centered on the specular angle with eccentricity e , defined by

$$f_s(\hat{k}_i, \hat{k}_r) = \frac{1}{4\pi} \rho_s(\theta_i, \lambda) \frac{h(\alpha)}{H(\theta_i) \cos \theta_r}$$

where

$$h(\alpha) = \frac{1}{(e^2 \cos^2 \alpha + \sin^2 \alpha)^2}$$

with α being the angle between the glint vector and the surface normal

$$\hat{g} = (\hat{k}_r - \hat{k}_i) / \sqrt{2(1 - \hat{k}_i \cdot \hat{k}_r)}$$

$$\cos \alpha = \hat{g} \cdot \hat{n}$$

and the normalization factor being

$$H(\theta_i) = \frac{1}{2e^2} [(1 - e^2) \cos \theta + \frac{2e^2 + (1 - e^2)^2 \cos^2 \theta}{(1 - e^2)^2 \cos^2 \theta + 4e^2}]$$

Thus, the four SR model parameters are:

$$\begin{aligned} \rho_D(\lambda) &= \text{diffuse spectral reflectance} \\ \mathcal{E}(\lambda) &= \text{spectral emissivity} \\ b &= \text{grazing angle reflectivity} \\ e &= \text{width of specular lobe} \end{aligned}$$

with an additional constraint for defining the energy in the specular lobe

$$\rho_s(\lambda) = G(b) - \rho_D(\lambda) - \mathcal{E}(\lambda)$$

The spectral parameters and the b parameter are usually fit to spectral, angular (10 to 80 degrees) HDR measurements and the e parameter is fit to in-plane BRDF measurements.

OPTASM BRDF model

The OPTASM BRDF model takes a somewhat more general approach to representing the BRDF in that the angular characteristics are specified by a number of Lorentzian shaped peaks. This provides flexibility in representing non-isotropic surfaces, which have peaks of scattered energy in non-specular directions. Typically, the BRDF is represented by two peaks, each defined by three parameters: the peak strength, A , the peak width in degrees, B , and the peak direction, \hat{k}_p , plus a constant term, ρ_o . (For isotropic materials, the ϕ_r location of the peak is assumed to be 180° from ϕ_i .) Thus, the BRDF is given by

$$\rho'(\hat{k}_i, \hat{k}_r) = \rho_o + A_1 / \{B_1^2 + 1 - \cos \Gamma_1\} + A_2 / \{B_2^2 + 1 - \cos \Gamma_2\}$$

where, $\Gamma = \cos^{-1}(\hat{k}_p \cdot \hat{k}_r)$, is the angle between the peak direction and the viewed direction.

One of the terms in this equation is used to represent the diffuse characteristic of the BRDF at grazing angles (similar to the SR b parameter) and the other term represents the main scattering lobe (similar to the SR e parameter) resulting in a seven parameter fit to the data. The parameters are fit to in-plane BRDF measurements using a Levenberg-Marquardt non-linear least-squares algorithm, and the peak strength parameters are then normalized to separate HDR measurements.

The flexibility of the OPTASM BRDF model lies in the fact that additional sets of parameters can be defined to represent more complicated scattering phenomenology. For example, many surfaces exhibit a distinct backscattering lobe and a bifurcation/shift of the forward scattering lobe from the specular direction for grazing incidence. Including additional Lorentzian lobes to the fitting function can represent these features.

Gaussian BRDF model

In applications requiring the BRDF for large numbers of (\hat{k}_i, \hat{k}_r) , for example, when integrating over large solid angles or in rendering for the production of physically accurate images, it is helpful to develop a model of the database which rapidly computes $\rho(\hat{k}_i, \hat{k}_r)$ with data files of manageable size.

The methodology of choice for accomplishing this depends on the degree to which rapidly varying lobes are present. If the scatterer is diffuse, so the BRDF is slowly varying, then a coarse sampling grid may be used for all four angles, which results in a database of manageable size. This database may then be directly interpolated.

However, if lobes of small angular subtense are present, the above procedure results in unreasonably large data files. For example, sampling all four angles at one-degree increments, which may well be required if specular features are present, results in about 10^9 floats. In this case, a “tracking” procedure is utilized. The tracking program operates in several modes. If the programmed angular increment in θ_i or ϕ_i loses contact with the lobe, a smaller increment, which may drop to one degree, is tried until the lobe is reacquired. If this fails, the user runs another utility to determine if the lobe truly vanished, and if so, where it reappears. This process constitutes the most difficult, time consuming and least automatic aspect of the entire project.

As flexible as the OPTASM model is in matching certain lobe structures, it has a disadvantage when applied to large databases involving large numbers of (\hat{k}_i, \hat{k}_r) . The seven OPTASM parameters are matched to the lobe data by the non-linear, least squares Levenberg-Marquardt method. This method is very effective in single instances, but convergence is slow, requiring many iterations. Furthermore it is difficult to program an automatic method that will determine the minimal number of iterations necessary to guarantee sufficient accuracy for numerous incoming directions.

To remedy this problem, a model was sought which can be fit to the data by performing computations in the “forward direction”. This means a single calculation is performed on the data, which results in the determination of the model parameters, thus obviating the necessity of executing many iterations of a successive approximation technique.

Though a number of different such models were examined, the Gaussian model,

$$\rho'(\hat{k}_i, \hat{k}_r) = A e^{-\tau}$$

where

$$\tau = a(\theta_i - \bar{\theta}_i)^2 + 2b(\theta_i - \bar{\theta}_i)(\phi_i - \bar{\phi}_i) + c(\phi_i - \bar{\phi}_i)^2,$$

has the advantage of possessing finite second moments,

$$\mu_{xx} = \int x^2 e^{-\tau} dx dy = \pi c / d,$$

$$\mu_{yy} = \int y^2 e^{-\tau} dx dy = \pi a / d,$$

$$\mu_{xy} = \int xy e^{-\tau} dx dy = -\pi b / d,$$

where

$$d = 2(ac - b^2)^{3/2}.$$

To use this model, all moments of the BRDF data up to the second are computed and equated to the corresponding Gaussian moment. The first moments determine $\bar{\theta}_r$ and $\bar{\phi}_r$. The lobe maximum determines A. The second moments determine a, b and c via,

$$a = \mu_{yy} \mu / d$$

$$b = -\mu_{xy} \mu / d$$

$$c = \mu_{xx} \mu / d$$

where this time,

$$d = 2(\mu_{xx} \mu_{yy} - \mu_{xy}^2)$$

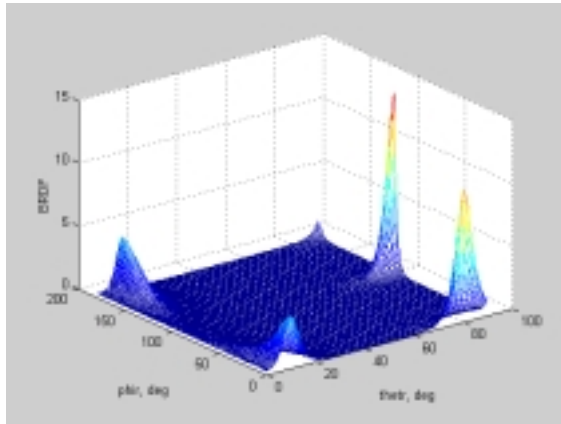
and

$$\mu = \int e^{-\tau} dx dy = \pi / \sqrt{ac - b^2}$$

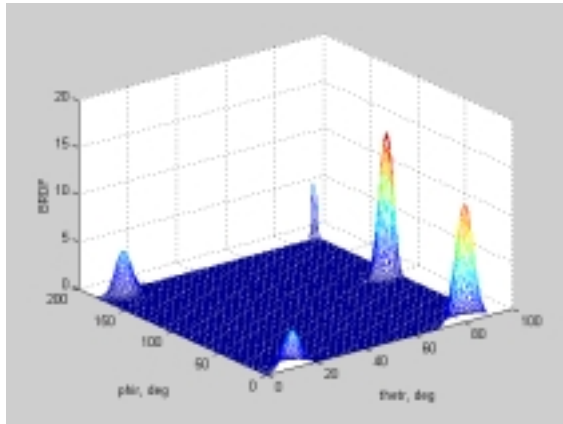
is the zeroth moment.

As stated above, for each incoming direction, the position of all lobes is “tracked”, and the above calculations performed to determine the six model parameters: $A, \bar{\theta}_r, \bar{\phi}_r, a, b, c$ as functions of (θ_i, ϕ_i) . When the four angles are input to the model, this secondary database is interpolated with (θ_i, ϕ_i) to get the six parameters, and these, with (θ_r, ϕ_r) in the Gaussian, yield the BRDF. While the same approach could be tried with the OPTASM model, no closed form expressions for the moments are known.

Figures 3 and 4 show the BRDF surfaces for two incoming directions as computed by Surface Optics’ MicroOpt program and the corresponding Gaussian model approximations.



(a)



(b)

Figure 3. (a) MicroOpt and (b) Gaussian model for $\theta_i = 10$ and $\phi_i = 0$.

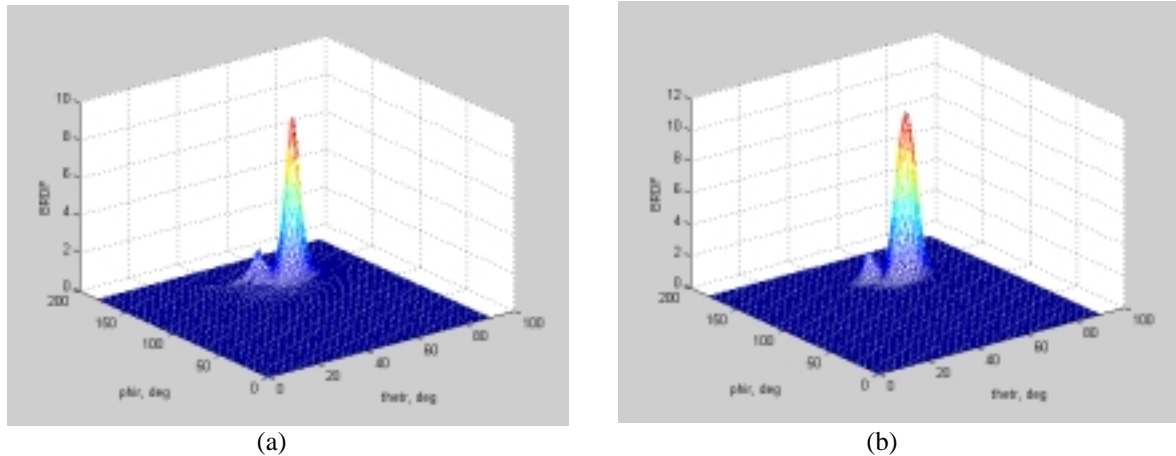


Figure 4. (a) MicroOpt and (b) Gaussian model for $\theta_i = 50$ and $\phi_i = 40$.

4.0 BRDF MEASUREMENTS

Accurate BRDF measurements for signature analysis requires a systematic mapping of the light scattered in the hemisphere. A recent paper by Thomas, *et al* [4] describes the laboratory and field Bi-Directional Reflectometers (BDR) at TACOM and CDNSWC that are used to perform these measurements. Figure 5 shows the in-situ BRDF system in use at TACOM for performing laboratory and field measurements

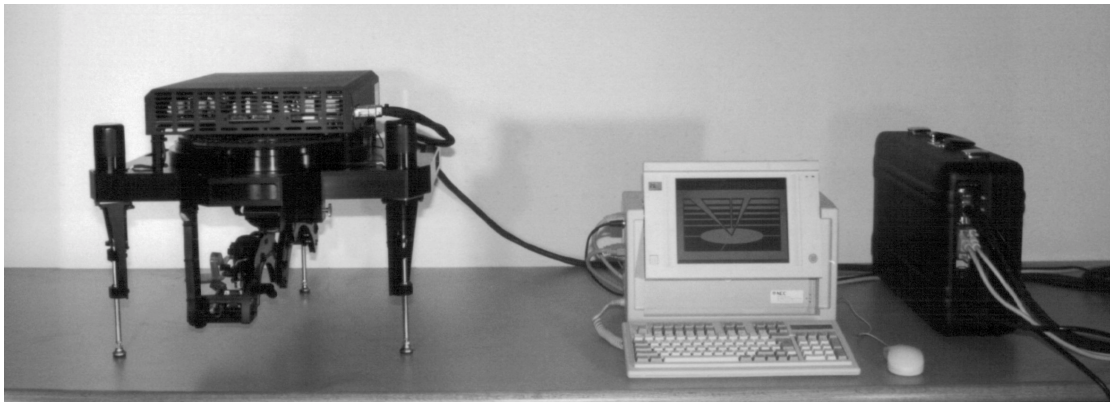


Figure 5 SOC-250 In-Situ Bidirectional Reflectometer.

This device and the support components are portable and can be brought to the field for extended measurement trials. An innovative light source and detector system allows for operation in an outdoor environment without special experimental set-up. This provides the ability to easily determine the BRDF of real world coatings and surfaces without extensive sample preparation and handling. Currently the instrument uses a quartz-halogen light source and CVF filter and avalanche photodiode detector for 10 nm spectral resolution between 0.4 to 1.2 microns. We are in the process of upgrading this instrument for spectral coverage to 14 microns. The recent paper by Beecroft and Mattison [5] provides a detailed description of the capabilities of this instrument.

Army Green 383 camouflage paint was used for this study. A complete set of angular HDR measurements and a reduced set of BRDF measurements (in-plane/cross-plane/ring data) were taken at Surface Optics Corporation and were used to fit the OPTASM and SR BRDF models.

In addition, a full hemispheric BRDF measurement of a different Green 383 sample was taken at TACOM as an independent data set for comparison to the parameterized models. Figure 6 shows a three dimensional plot of the BRDF of Green 383 at a wavelength of 0.5 microns and 50° incident angle.

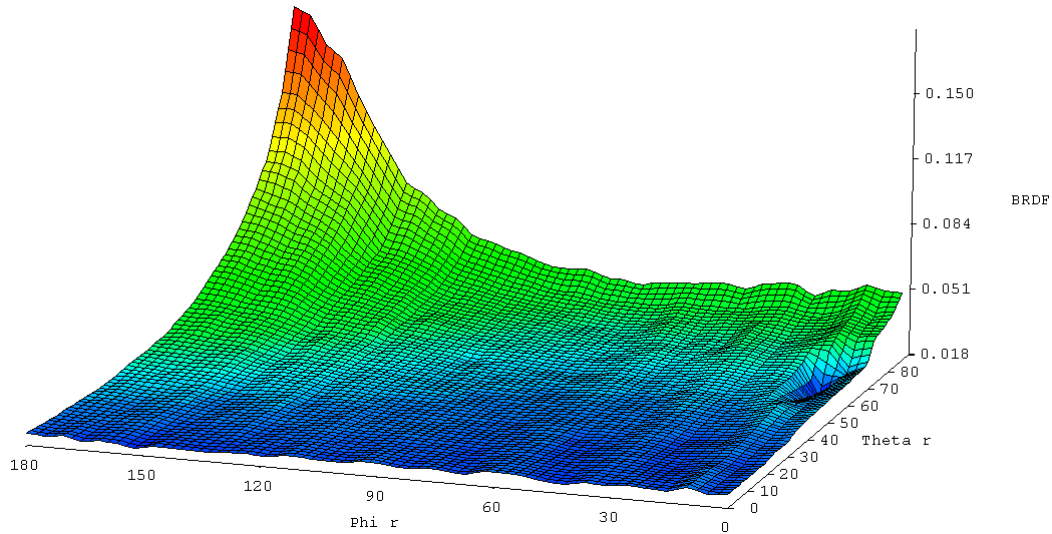


Figure 6 BRDF of Army Green 383 at 0.5 Microns and 50° Incident Angle.

5.0 MODEL-MEASUREMENT COMPARISON

In-plane BRDF measurements and angular HDR measurements of Green 383 were used to fit the SR model parameters. The BRDF measurements were taken at 0.54, 4.44 and 10.0 microns. These three bands were selected to capture the important scattering features in the VIS/NIR, MWIR and LWIR spectral bands.

Sandford-Robertson BRDF model results

The SR model fitting procedure involves fitting the $\epsilon(\lambda)$ and b parameters to the spectral HDR measurements. The b parameter is obtained from equation (4) by averaging the ratio of the near normal measurement to the measurements from 50 to 80 degrees. The $\rho_D(\lambda)$ and e parameters are obtained by iteratively adjusting the energy in the specular lobe and the shape so that a reasonable fit is achieved for each of the three incident angles (20, 40 and 60 degrees). The results of the SR model fit are shown in Figures 7–9 for 0.54, 4.4, and 10 microns respectively.

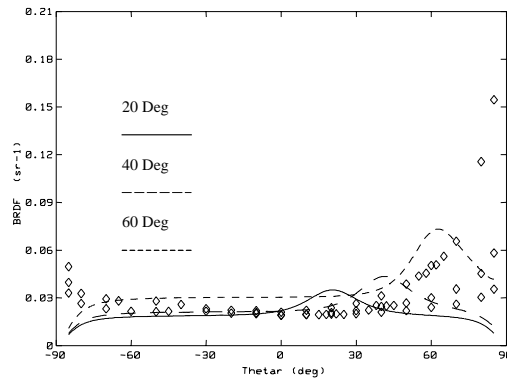


Figure 7 SR BRDF Fit to Army Green 383 at 0.54 Microns.

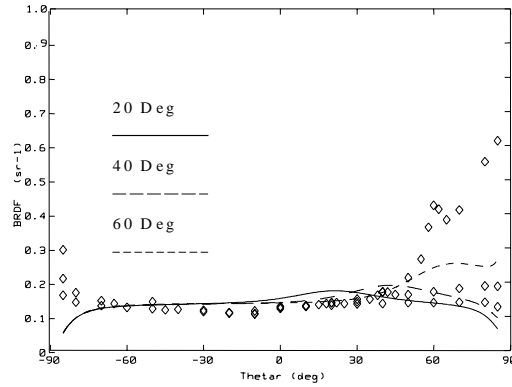


Figure 8 SR BRDF Fit to Army Green 383 at 4.44 Microns.

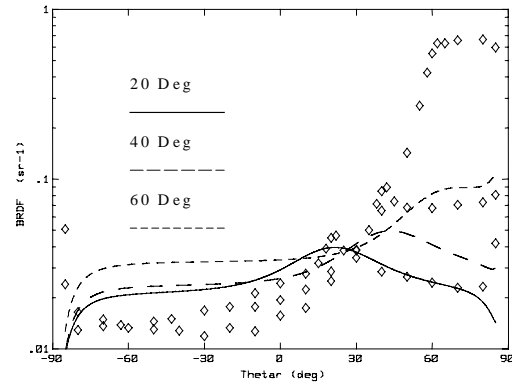


Figure 9 SR BRDF Fit to Army Green 383 at 10.0 Microns (Note Log Scale).

The SR model results shown in Figures 7-9 do not show very good agreement with the data. Since the fitting process involves human judgement on what defines a “good fit” other analysts would produce different fits to the data. Our criteria was to choose SR parameters that qualitatively look the best for all three incident angles. A better approach would be to obtain the best fit for a specific input angle, e.g., 40°, which has the most impact on the signatures because of the solid angle weighting.

Another factor is that the analytic form of the SR model is simply not well suited to very diffuse paint systems. The grazing angle scattering that is characteristic of this type of coating cannot be modeled by circular ellipsoid lobe fixed at the specular direction. Table 1 gives the SR model parameters that were obtained from this analysis.

Table 1 SR Model Fitting Parameters for Army Green 383.

λ (μM)	$\rho_D(\lambda)$	$\varepsilon(\lambda)$	B	E
0.54	0.1357	0.8598	0.119	0.159
4.44	0.4108	0.5630	0.119	0.250
10.0	0.1025	0.8856	0.119	0.249

OPTASM BRDF model Results

The OPTASM BRDF model parameters were fit to the in-plane/cross-plane and ring BRDF measurements at three incident angles (20° , 40° and 60°) and three wavelengths (0.54, 4.4, and 10 microns). The HDR measurements for each incident angle and wavelength were then used to renormalize the strength parameters. The fitting procedure iteratively calls a Levenberg-Marquardt non-linear least squares fitting algorithm to adjust the parameters. The analyst monitors the chi-squared (goodness-of-fit) parameter and the graphic BRDF display until a satisfactory fit is obtained.

The results of fitting the OPTASM BRDF model are shown in Figures 10–12 for 0.54, 4.4, and 10 microns respectively. The fit for the OPTASM BRDF model appears much better than the SR model, particularly in capturing the grazing angle dependence for high incident angles (Figure 12). However, because the model parameters were fit at each incident angle, the comparison is between a 21-parameter model and a 4-parameter model at each wavelength.

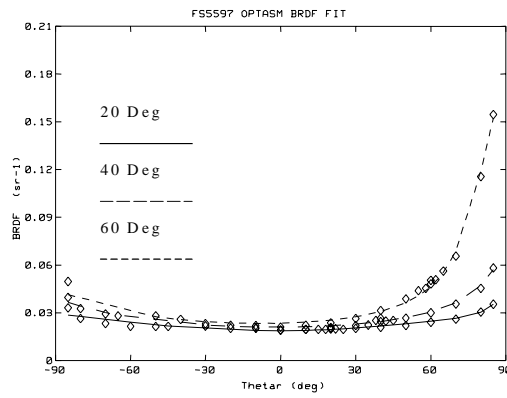


Figure 10 OPTASM BRDF Fit to Army Green 383 at 0.54 Microns.

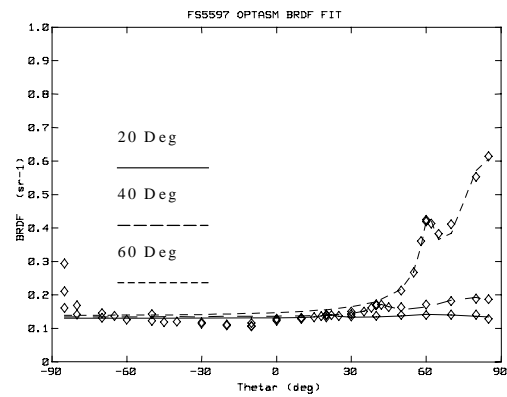


Figure 11 OPTASM BRDF Fit to Army Green 383 at 4.4 Microns.

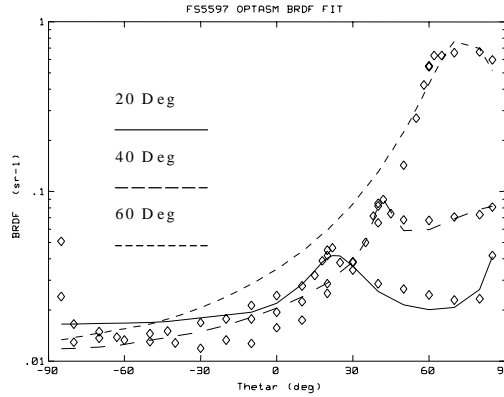


Figure 12 OPTASM BRDF Fit to Army Green 383 at 10 Microns (Note Log Scale).

Table 2 gives the OPTASM model parameters that were obtained from this analysis. Note that some of the fit parameters are negative. This is an artifact of the numerics and the parameters in this case have no physical interpretation. Evaluation of the BRDF for an arbitrary incident angle involves interpolation/extrapolation of the model parameters from the incident angles used for the fit.

Table 2 OPTASM Model Fitting Parameters for Army Green 383.

λ	Fit Param	θ_i		
		20	40	60
0.54	ρ_o	0.224	0.0	0.0
	θ_{p1}	83.2	105.7	185.1
	A_1	4.74e-5	6.81e-3	7.85e-2
	B_1	2.06e-2	5.74e-0	1.3e+1
	θ_{p2}	-2.0	-175.6	88.5
	A_2	-6.6e-1	7.38e-2	1.61e-2
	B_2	-2.4e+2	2.5e+2	8.87e-0
4.44	ρ_o	0.130	0.133	0.132
	θ_{p1}	21.0	41.7	60.7
	A_1	5.50e-4	2.35e-3	6.42e-3
	B_1	2.4e+0	3.48e-0	2.56e-0
	θ_{p2}	62.6	77.3	84.0
	A_2	3.89e-3	1.56e-2	7.67e-2
	B_2	1.1e+1	1.2e+1	9.57e-0
10.0	ρ_o	0.016	0.0	0.0
	θ_{p1}	23.2	41.8	73.8
	A_1	1.02e-2	3.85e-3	1.94e-1
	B_1	8.8e+0	3.30e-0	1.0e+1
	θ_{p2}	92.6	92.3	85.0
	A_2	1.21e-3	7.57e-2	9.94e-5
	B_2	1.3e+0	3.3e+1	1.0e+1

Figure 13 illustrates some of the complex scattering phenomenology exhibited by paint systems that challenge the capabilities of parameterized BRDF models. The figure shows the in plane BRDF of Green 383 at 4.44 microns for 40° incidence compared to the OPTASM BRDF model fit.

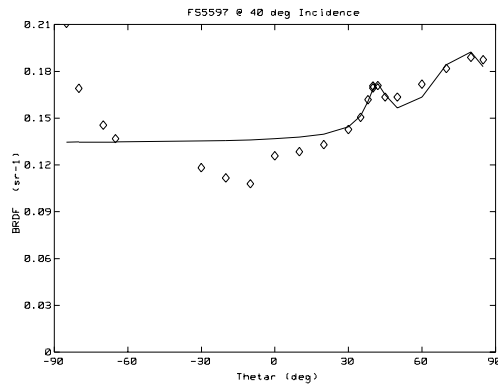


Figure 13 OPTASM BRDF Fit Illustrating the Complex Scattering Phenomenology from Paint Systems.

Note the increase in the forward and back scattering at grazing angles, the specular peak and a significant decrease in the scattering at angles near normal. A three or four term OPTASM fit to this data would significantly increase the fidelity of the fit at the expense of added computational complexity.

Comparison with TACOM measurements

As a test of the OPTASM BRDF parameterization we compared the model predictions to an independent set of data, which was shown in Figure 3. The TACOM in-plane data at 0.5 microns for 50° incident angle is shown in Figure 14, compared to the in-plane data taken at 0.54 microns for 40° and 60° incident angles. The comparison is between measurements taken on two different reflectometers of two different samples of Green 383, and shows a good agreement between the measurement systems.

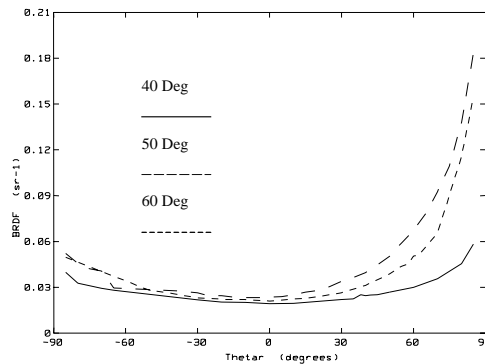


Figure 14 Comparison of TACOM Measured BRDF at 50 Degrees to the In-Plane Measurements at 40 & 60 Degrees.

Figure 15 shows a comparison between the OPTASM BRDF model prediction at 50° to the TACOM measurements. The BRDF prediction used the 21-parameter fit at 0.54 microns shown in Table 2. The odd shape of prediction is explained by the wild variations and inconsistency of the fitted peaks found for 20-, 40-, and 60-degree incident data. That is, the non-physical (negative) model parameters generated by the fitting process are not well suited for interpolation/extrapolation to other angles in this case.

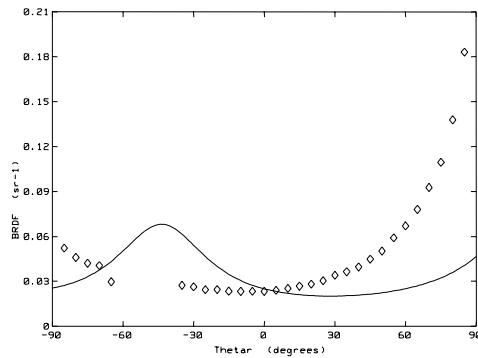


Figure 15 Comparison of the OPTASM BRDF Model Prediction at 50 Degrees to the Measurements.

A more constrained and user-guided fitting process would no doubt cure this - something that will be investigated in the future given the demonstrated capability of Levenberg-Marquardt for extremely good fits of the actual data.

A much better result was obtained using the MWIR parameters. Figure 16 shows the OPTASM BRDF prediction at 4.4 microns for 50° compared to the model fits at 40° and 60°. This shows more regularly evolving peaks, and demonstrates the important potential of this OPTASM parameter interpolation approach.

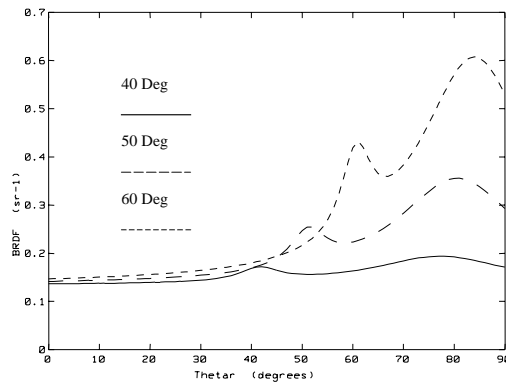


Figure 16 OPTASM BRDF Model Prediction for 50 Degrees at 4.4 Microns.

6.0 SIGNATURE ANALYSIS

The radiometric effects of these parameterized BRDF models are assessed using signature predictions produced by the ENSIR and OPTASM signature analysis codes.

The ENSEmble of InfraRed (ENSIR) analysis codes includes a full transient thermal analysis model, LOWTRAN7/MODTRAN atmospheric radiance codes, simplified plume analysis and a radiance mapper for producing pixelized images. The radiance calculation interpolates from a full BRDF and HDR measurement data set and generates visible and IR radiometric images using the algorithms embodied in the Optical Signatures Code (OSC).

The Optical Target Signature Model (OPTASM) was developed by C. Acquista and R. Rosenwald [6] of PAR Government Systems for Jon Jones at USAF Rome Laboratories. This code also uses LOWTRAN7/MODTRAN for atmospheric calculations, but has a limited thermal analysis capability because it was developed primarily for fixed wing aircraft applications. The code features extensive capabilities for radiometric calculations, including exploiting the capabilities of the Lorentzian lobe BRDF model for general non-isotropic, polarizing surfaces.

We investigated the radiometric effects of these parameterized BRDF models by performing comparisons between OPTASM and ENSIR signature simulations on a flat panel for near normal (20°) and near grazing (70°) solar illumination geometries. Figure 17 defines the scenario of the simulation.

Spectral Bands:	Vis (0.49-0.51 μm); MWIR (3-5 μm)
Geometry:	20° Sun, 20° Obs; 70° Sun, 70° Obs 1 km Slant Path
Atmosphere:	1962 Standard, Rural Aerosol/23 km
Skyshine:	18 Elevations (5°), 8 Azimuths (45°)
Panel Area:	1 m ²
Panel Temp:	295 K
Panel Orientation:	Horizontal, 2 m Above Ground

Figure 17 Scenario Used for Signature Simulations.

The ENSIR model interpolates the BRDF from a measurement database, and was used to generate signatures using the SR model by generating a full hemispheric database from the SR parameters. ENSIR was also used to generate the signatures from the BRDF data using the in-plane, cross-plane and ring measurements, and the TACOM full BRDF measurements where appropriate.

The results of the visible band signature analysis calculations are shown in Table 3, and the results for the MWIR band are shown in Table 4. The BRDF column indicates signatures generated using the measurements directly (Data), the Sandford-Robertson model (SR) and the OPTASM BRDF model (OPT). The Data and SR calculations were performed using ENSIR and the OPT calculations were performed using OPTASM Version 2.1.24. All values tabulated are inherent (at the target) intensity (w/sr) values.

Table 3 Comparison of Signature Analysis Calculations (w/sr) in the Vis Band for Different BRDF Models.

Angle	BRDF	Ref Sol	Ref Sky	Emis	Total
20	Data	0.277	0.133	0.0	0.410
	SR	0.677	0.297	0.0	0.974
	OPT	-2.761	1.910	0.0	-0.851
70	Data	0.047	0.052	0.0	0.099
	SR	0.072	0.061	0.0	0.133
	OPT	0.067	0.091	0.0	0.158

Table 4 Comparison of Signature Analysis Calculations (w/sr) in the MWIR Band for Different BRDF Models.

Angle	BRDF	Ref Sol	Ref Sky	Emis	Total
20	Data	1.123	0.166	0.958	2.248
	SR	1.381	0.281	0.958	2.620
	OPT	1.280	0.275	0.851	2.420
70	Data	0.446	0.112	0.308	0.865
	SR	0.216	0.093	0.308	0.616
	OPT	0.291	0.143	0.271	0.705

In the tables, the differences between the Data and SR results can be explained in terms of the quality of the fit as exhibited earlier. In the Vis band the OPT model results are in reasonable agreement, except for the Vis 20° case, where the interpolation between the wildly varying parameter sets is undoubtedly the explanation. Although there is a difference in the self-emission terms in the MWIR between OPTASM and ENSIR, the OPT results are much more reasonable, because the interpolation is stable, as illustrated by the discussion in connection with Figure 16.

Looking at the reflective terms only, and making the assumption that the Data result is the “true” value, discrepancies between the OPTASM and SR BRDF models and the Data lead to signature “errors” approaching 60% in some cases. This could have a significant impact on the system level evaluation of a LO surface treatment.

7.0 CONCLUSIONS

The results of this study suggest that the widely used Sandford-Robertson model is not the best choice for representing the BRDF of very diffuse paint systems. The assumptions of the analytic form of the specular lobe and the grazing angle reflectivity are not well suited to model the complex multiple scattering phenomenology that is characteristic of diffusely scattering surfaces.

The OPTASM BRDF model also has difficulty with very diffuse coatings that exhibit significant grazing angle scattering. The Lorentzian lobe parameters do a reasonable job fitting the measured data, but non-physical (i.e., negative) model parameters that can occur for very diffuse coatings show poor results when they are interpolated/extrapolated to other incident angles. A more constrained fitting procedure might help to alleviate this problem.

In general, the OPTASM BRDF model is much more flexible because the number and shape of the Lorentzian lobe parameters can be adjusted to fit both diffuse and specular scattering. Also, the direction of the scattering lobes are not constrained to be at the specular position which is better for representing the grazing angle gloss feature observed in many paint systems, as well as the small forward shift of the specular peak sometimes observed for moderately specular coatings. However, the large number of parameters required for accurate representation of the measured data (nominally, 21 parameters for the case presented here) negate some of the advantages of going to a simplified BRDF model in the first place.

When reflectance models are used in comparative signature calculations on simple flat panel targets, the ability of a given model to extrapolate to other directions is put to test. Restriction of certain BRDF models to certain codes, e.g., the OPTASM BRDF model, limits our ability to conclusively test those models. The ENSIR code, accepting any model BRDF's provided they are in measurement format, represents a good test bed because it can provide a direct comparison to measured BRDF data. This eliminates the uncertainties introduced through algorithmic differences between the various signature analysis codes.

Given the ongoing development and application of LO surface treatments the ability to evaluate the effect of surface BRDF on signatures will become increasingly more important. The availability of automated bi-directional reflectometer instruments readily provides the BRDF measurement data, and it is clearly of interest to develop BRDF representations to exploit this data for signature analysis. However, it is also clear from the results of this simple case of a diffuse paint system on a flat plate that more work needs to be done in developing and validating BRDF model parameterizations if they are to be used for quantitative evaluation of surface treatments.

ACKNOWLEDGEMENTS

The authors would like to thank Jim Crosby of TACOM for assistance in making the BRDF measurements.

REFERENCES

1. F. Nicodemus, "Directional Reflectance and Emissivity of an Opaque Surface", *Appl. Opt.*, **4**, pp. 767-773 (1965).
2. B. Sandford and D. Robertson, "Infrared Reflectance Properties of Aircraft Paints," *IRIS Targets, Backgrounds and Discrimination* (1985).
3. C. Acquista and R. Rosenwald, "Multiple Reflections in Synthetic Scenes," *Proceedings of the Fifth Annual Ground Target Modeling & Validation Conference*, Houghton, MI (1994).
4. D. Thomas, J. Jafolla and P. Sarman, "Bidirectional Reflectance Measurements for High Resolution Signature Modeling," *Proceedings of the SPIE Symposium on Targets and Backgrounds: Characterization and Representation III*, Orlando, **Vol. 3062**, 105-116 (1997).
5. M. Beecroft and P. Mattison, "Design Review of an In-Situ Bidirectional Reflectometer," *Proceedings of the SPIE Symposium on Surface Scattering*, San Diego, Vol. 3141, (1997).
6. C. Acquista and R. Rosenwald, "Software User's Manual for the Optical Target Signatures Model (OPTASM) Version 2.1," (available from) *Surface Optics Corporation* (1993).